Formation and Inflammation of a Turbulent Jet

A. F. Ghoniem*
Massachusetts Institute of Technology, Cambridge, Massachusetts
D. Y. Chen†
Allison Gas Turbine Operations, Indianapolis, Indiana
and
A. K. Oppenheim‡
University of California, Berkeley, California

The formation and inflammation of a planar, turbulent jet in an incompressible medium is modeled numerically by the use of the random vortex method amended by a flame propagation algorithm. The results demonstrate the dominant influence of the dynamics of turbulent eddies upon the development of the jet. Its growth is shown to consist of three stages: formation of small eddies, pairing of eddies with the same sign of circulation, and pairing of eddies of opposite signs. On this basis, a number of features of the jet mechanism are revealed, namely, penetration, engulfment, entrainment, and intermittency. Two cases of inflammation are considered. In one, the jet is ignited at the center of the orifice, the solution tracing its own inflammation. In the other, combustion is initiated across its full cross section, the results modeling the action of a turbulent torch as it spreads the flame into the combustible surroundings. In both cases, the flowfield is still dominated by the turbulent eddies and their interactions. However, the coherence among them is encumbered as a consequence of expansion due to the exothermicity of combustion.

Introduction

THIS paper reports on the theoretical part of a general program of research on flame and plasma jet ignition systems. The experimental results have been reported elsewhere.[1-4] The purpose of this paper is to provide insight into the generating mechanism of the phenomena whose outward manifestations were described in Refs. 1-4.

A more detailed account of this work is provided in a report published by NASA.[1] The problem considered here is that of the formation and inflammation of a turbulent jet. The computations are based on the use of the random vortex method developed by Chorin[5-7] and extended by us[8,9] in collaboration with Chorin[10] to include the effect of combustion. Recently, Majda[11] furnished a rigorous derivation of equations for low Mach number combustion, proving the validity of our formulation provided that the dimension of the domain of interest is sufficiently large with respect to flame thickness and that the Mach number of the flow is very low, as is indeed the case here.

The subject matter of our work is, of course, closely related to the study of the large-scale structure of turbulent shear layers, launched by the pioneering work of Brown and Roshko and their collaborators.[12-15] Of particular relevance to the problem at hand are the papers of Papailou and Lykoudis[16] on the mechanism of entrainment in a turbulent wake, and of Browand and Laufer[17] on the influence of large-scale eddies upon the formation of circular jets.

Theoretical studies in this field were based primarily on numerical analysis. They were particularly helpful in revealing that vorticity, as a result of the Kelvin-Helmholtz instability, tends to conglomerate, forming large-scale eddies (see, e.g., Patnaik et al.[18] and Corcos and Sherman[19]), which grow by entraining fluid from the surroundings and by pairing—the basic mechanism of the growth of the shear mixing layer. Among the numerical techniques used for this purpose, the most prolific are vortex methods because of their capability to trace small vortex elements as they interact, forming eddy structures, without any artificial restriction upon their motion or distortion due to numerical diffusion that is *perforce* introduced in finite difference schemes. Thus, Ashurst[20] was able to provide a numerical simulation of the experimental observations of Brown and Roshko[11] by the use of the random vortex algorithm of Chorin,[5] with a suitable modification of the vorticity field of each element to obtain a successful reproduction of results. Delcourt and Brown[14] used a "vortex-in-cell" algorithm to study the evolution of infinite layers of vorticity and thereby rationalize the experimentally observed growth of the shear layer.

The random vortex method acquired a solid foundation as a consequence of the contributions of Hald[21] who, in collaboration with Del Prete,[22] proved that its solution converges with second-order accuracy to that of the inviscid Euler equations for rotational flow over an arbitrarily long time. Thus, the discretization error in the numerical solution decays at a rate inversely proportional to the number of vortices used in the calculations. Subsequently, Beale and Majda[23] demonstrated that higher order schemes can be devised by proper choice of vorticity distribution within a vortex element. At the same time, they proved the validity of viscous splitting schemes, that is, treating the Navier-Stokes equations in two fractional steps, first as the Euler equation and second as a diffusion equation.[24] Thus, they provided the essential background for the use of random walk to simulate the diffusion of vorticity in a Lagrangian frame of reference.

Following is a concise description of the random vortex method and its application to turbulent combustion, as well as of two essential modifications necessitated by the unbounded flowfield of the free jet under study. The results obtained on this basis are then presented and discussed, concerning first the formation of a turbulent jet and then its inflammation. All of these results pertain to planar, strictly two-dimensional flow. Two cases of inflammation are considered. In one, the

Presented as Paper 84-0572 at the AIAA 22nd Aerospace Sciences Meeting, Reno, NV, Jan. 14-16, 1984; received Aug. 13, 1984; revision received April 9, 1985. Copyright © American Institute of Aeronautics and Astronautics, Inc., 1985. All rights reserved.

*Assistant Professor, Department of Mechanical Engineering.
†Senior Project Engineer.
‡Professor, Department of Mechanical Engineering.

jet is ignited at the center of the orifice. In the second, combustion is initiated across its whole cross section. Thus, the first traces the inflammation of the jet itself, while the second models the action of a turbulent torch in spreading the flame out into the surrounding combustible atmosphere.

Method

Computations are based on the random vortex method which, as pointed out in the introduction, has been especially expanded to treat turbulent combustion systems. The method provides a fundamental solution of the time-dependent, incompressible Navier-Stokes equations at high Reynolds numbers without averaging or resorting to turbulence closure modeling.

Whereas our previous publications[9,25] dealt with the fundamental aspects and operational details, salient features of the algorithm are presented here with reference to the block diagram in Fig. 1. As evident there, the velocity vector is evaluated as a sum of two components: u_ξ obtained by the *vortex dynamics* calculation and u_ϵ by the use of the *flame propagation* algorithm.

The first is treated on the basis of the Navier-Stokes equations expressed in terms of vorticity transport, describing an essentially solenoidal field of the diffusion and convection of vorticity $\xi(x,y)=\partial v/\partial x-\partial u/\partial y$. Its distribution is discretized, forming an interacting set of vortex elements, the so-called vortex blobs. A vortex blob is defined as an element of vorticity of a small but finite core. Within the core of a blob, vorticity is finite, while outside the core, vorticity is zero. If the core is taken as zero, the blob becomes a potential vortex; thus creating an infinite velocity at the center and resulting in numerical instabilities. The situation is remedied by using finite cores with smooth distribution of vorticity. The Kelvin-Helmholz theorem is satisfied by keeping the vorticity and circulation associated with each blob constant as it moves through the field. More details are given in Refs. 5 and 9.

Each elementary blob affects all the other blobs by a Biot-Savart effect of its own velocity field. Vortex blobs are continuously generated at the walls to satisfy the no-slip boundary conditions $u\cdot s=0$. In the computations, this is implemented by a numerical boundary layer, where the blobs are reduced to one-dimensional vortex sheets, modeling the distribution of $\xi(x,y)=-\partial u/\partial y$. At each time step, every blob is displaced by convection due to the Euler component of the Navier-Stokes equations, while the process of diffusion is simulated by random walk governed by a set of Gaussian variables with zero mean and a variance of $2k/Re$, where k is the time step and Re is the Reynolds number of the flowfield.

The second component of the algorithm is associated with the propagation of the flame, which is treated computationally as a thin line interface between reactants and products according to the thin flame model. Its motion produces an essentially irrotational field associated with expansion due to the jump in specific volume, modeled by a line of sources

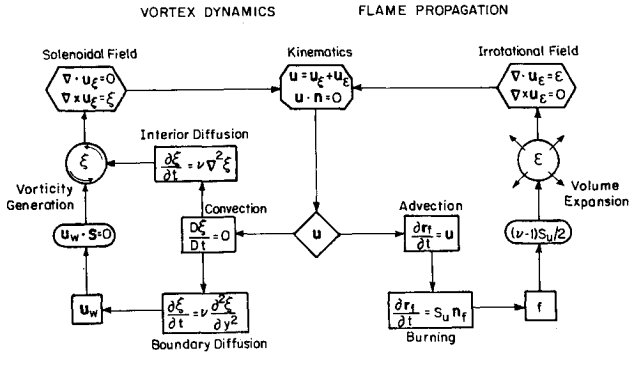

Fig. 1 Block diagram of the algorithm.

delineated by the front. Their strength per unit length of the front is $\epsilon=(\beta-1)S_u/2$, located at r_f: the position vector of the flame front, $\beta=v_b/v_u$, v denoting specific volume, while subscripts b and u denote the burnt and unburnt media, respectively, whereas S_u is the normal speed. The displacement of the flame front at each time step consists of three components: advection due to the velocity field in which it exists, self-advancement at a normal burning speed, and the aforementioned volumetric expansion, endowing it with dynamic properties. The calculations are carried out by the use of SLIC (simple line interface calculation), developed by Noh and Woodward[26] and amended by Chorin[10] to enhance its spatial resolution and implement the Huygens law in the self-advancement step (see Ref 27).

The essential difficulty associated with the numerical analysis of a free jet is due to the fact that its flowfield is unbounded. Thus, in contrast to a flow in a channel, where the balance between outflow of vortex elements, their generation in the interior, and their flux at the inlet leads to the establishment of a steady saturation state, the total number of vortex blobs increases indefinitely (see Ref. 1). As a consequence, the amount of elementary operations grows rapidly so that the CPU time soon becomes prohibitively large.

To deal with this difficulty, following the cloud-in-cell technique described by Baker[28] and Leonard,[29] we developed a "dipole-in-cell" method. Its basic features are as follows.

The field is divided into a number of square cells M, each with side width c. However, instead of distributing the vorticity in each cell among its four corners and resorting to a Poisson solver to evaluate the induced velocity as it is done in the cloud-in-cell technique, we replace all the vortex blobs in a cell by a dipole located at the centroid of the original vorticity and use it in updating the induced velocity in the far field.

Specifically, in the cell denoted by (i,j), if $\Gamma_{ij}^{\pm}$ is the strength of the equivalent dipole while $z_{ij}^{\pm}$ is its centers, then

$$\Gamma_{ij}^{\pm}=\Sigma\Gamma^{\pm}(z)$$

while

$$\begin{matrix} z_{ij}-c/2 & z_{ij}+c/2 \\ \leq z \leq & \\ z_{ij}-ic/2 & z_{ij}+ic/2 \end{matrix}$$

$$z_{ij}^{\pm}=\Sigma z\Gamma(z)/\Gamma_{ij}^{\pm}$$

where $z=x+iy$ is the complex coordinate and Γ is the circulation of a vortex blob. The first expression quarantees that the velocity field of the equivalent dipoles has the same total circulation as the original set of vortices. The second expression assures the conservation of the first moment of the vorticity field. In principle, the equivalent field should conserve all the moments of the original vorticity. However, the error introduced by neglecting moments of higher orders cannot be of essential significance, especially since the original discrete vorticity field itself does not satisfy the higher order moments of the continuous field it models.

The use of a dipole prevents the occurrence of a fundamental error that would have been made if the positive and negative vorticities were allowed to cancel each other. Such vorticities induce a field although their sum is zero. On the other hand, the velocity induced by a dipole decays as r^{-2}, while that of a vortex decreases only as r^{-1}. Consequently, long-range effects of a dipole are smaller. This discrepancy turns out to be of advantage when a cutoff radius of influence is introduced, as demanded by the accuracy of the computer. For example, since the error in calculating the velocity $|u|$ by a six-digit-accurate machine is of an order of 10^{-6}, then for $\Gamma\approx 10^{-2}$, it follows that R_c (vortex) $\approx 10^{-4}$ while R_c (dipole) $\approx 10^{-2}$, where R_c is the cutoff radius of influence for a flow element.

In the implementation of the dipole-in-cell method, the velocity at point z is calculated as a sum of two components, u_n as the near-field contribution due to all the vortex blobs

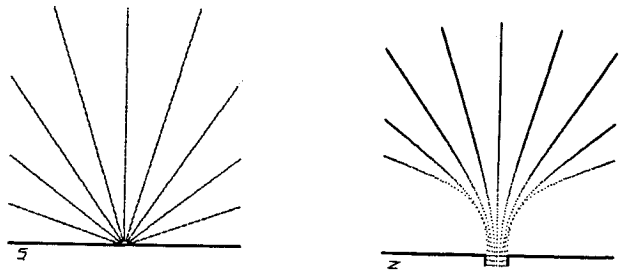

Fig. 2 Streamlines of potential jet in the physical z plane and the transformed ζ plane, representing the flowfield at zero time.

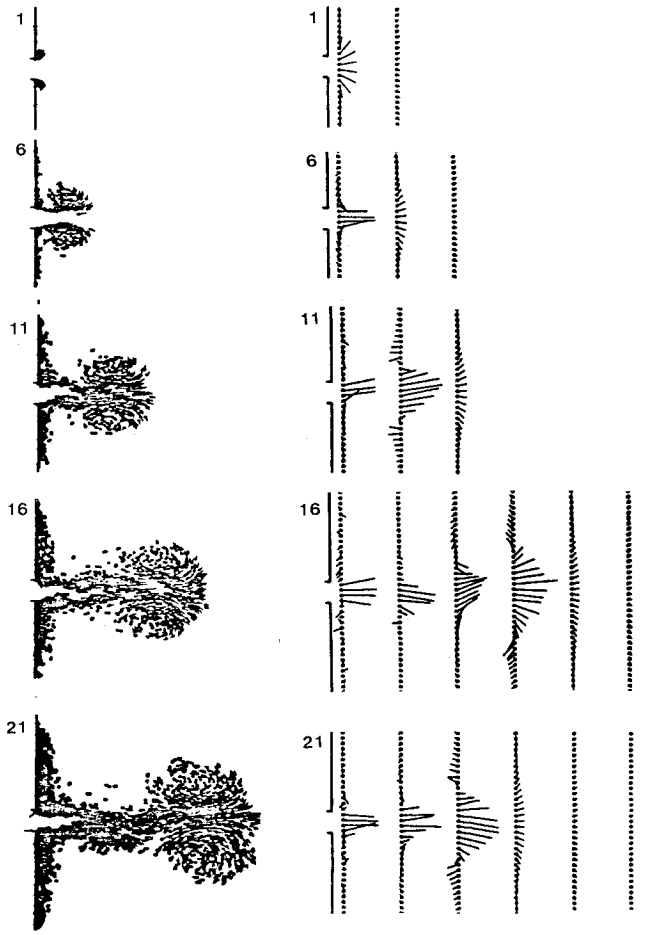

Fig. 3 Development of vorticity field and the corresponding velocity profiles of a turbulent jet issuing from an orifice at $Re = 10{,}000$; boundary layers at side walls considered. Numbers denote nondimensional time $T = u_j t/d$, where u_j is the inlet flow velocity, t the time, and d_j the orifice diameter.

located in the cell (i,j) as well as its eight neighbors, and u_f as the velocity introduced at z by the dipoles in the rest of the field. The operation count of this method is of an order of $(N_n^2 + M^2)$, where N_n is the number of vortex blobs in the near field and M is the number of dipoles in the remaining space. Comparison to $\mathcal{O}(N^2)$, where N is the total number of vortex blobs, reveals the gain in computational time. For a uniformly distributed vorticity field $N_n = N/M$ and the factor of saving is proportional to $(N^2 + M^2)/(NM)^2$. In general, however, the vorticity is not distributed uniformly. A judicious choice of the number and location of M cells is therefore required in order to optimize the benefit in CPU time to be gained by the dipole-in-cell method while minimizing the error introduced by the approximation.

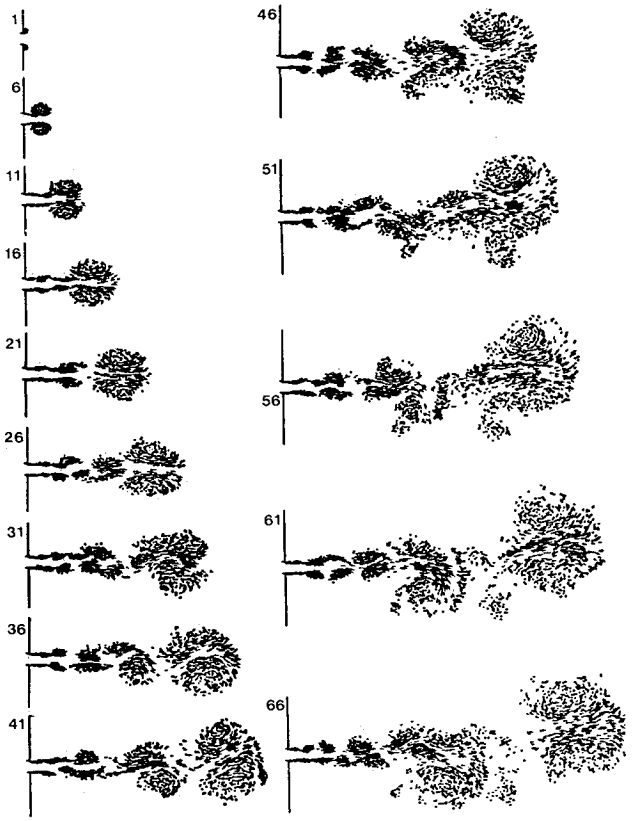

Fig. 4 Development of vorticity field associated with formation of a turbulent jet issuing from an orifice at $Re = 10{,}000$, effect of boundary layer at side walls neglected; numbers as in Fig. 3.

Jet

The representative case we considered is that of a free jet issuing from an orifice to a semi-infinite plane at a Reynolds number of 10,000, based on the orifice diameter of the jet, the incoming flow velocity, and its kinematic viscosity.

To start with, there is a potential flowfield. This is determined by conformal mapping, as shown in Fig. 2, presenting, on the left, the physical z plane and, on the right, the transformed ζ plane. The conformal transformation function used for this purpose is specified by the differential form

$$d\zeta/dz = \pi\zeta/\sqrt{\zeta^2 - 1}$$

The development of the vorticity field and the associated velocity profiles computed for the formation of a turbulent jet are depicted in Fig. 3. The display consists of a set of results selected at various instances of time, as marked on labels. The time is expressed in a nondimensional form: $T = u_j t/d$ where u_j is the inlet flow velocity, t is time, and d is the orifice diameter. Each diagram in the left column of Fig. 3 contains all the vortex blobs used in the computations up to its own time. The boundary layers on all the walls shown in the figure were taken into account via the numerical boundary-layer technique. As a consequence, the total number of vortex blobs grew rapidly, causing the CPU time to become excessively long after $T = 21$. At larger times even the saving obtained by the use of the dipole-in-cell method became insufficient. An introduction of a more drastic simplification became necessary, while the results obtained so far were retained as a proving ground for the validation of the simplified technique.

The simplification was simply attained by neglecting the effects of the boundary layer at the side walls, so that the turbulent jet was formed solely by the vorticity generated at the edge of the orifice. The vorticity fields obtained in this way are displayed in Fig. 4, while the corresponding velocity profiles

are presented in Fig. 5. These results appear to be in a satisfactory agreement with those of Fig. 3, whereas the number of vortex blobs has been significantly reduced. Although it took somewhat longer to grow to the same size, this allowed the computations to be continued for a sufficiently long time to display all the significant features of the formation of a free turbulent jet.

As revealed here, this process consists of three distinct stages:

1) In the first stage, presented by our graphical output in Fig. 4 up to $T=16$, a small eddy is formed due to the breakdown of the vorticity layer on the sides of the jet, caused by boundary-layer separation at the exit of the nozzle. Eddies produced at this stage are quite symmetric, recirculating in opposite directions without any discernible interaction between each other. All of them are of almost the same size, and they grow gradually as they move downstream while entraining the irrotational fluid from the surrounding atmosphere.

2) In the second stage, depicted in Fig. 4 by outputs at time interval $T=21-36$, eddies on each side of the jet start to pair, while their progress downstream slows down because their convection velocity is inversely proportional to their distance from the orifice. The interaction between eddies downstream is thereby enhanced, leading to the formation of pairs of intertwining eddies with the same sense of rotation. These eddies induce a circular motion of one around the other, causing a rotary flow of their fields around a common center. As a consequence, they fuse together, forming a larger eddy—the essential mechanism of pairing. The sequence of events constituting this process is clearly illustrated in Fig. 4 by the middle nodule on the bottom, leading to the formation of the penultimate eddy at $T=36$.

3) In the third stage, displayed in the rest of Fig. 4, the interaction between eddies of opposite sense of rotation induces motion transverse to the jet axis. Fundamentally, one would expect two counterrotating eddies to exert a unidirectional effect on each other, causing them to move in the direction normal to their line of centers, so that their trajectories are parallel. However, the small-scale motion due to diffusion obliterates the boundary between them, leading to a uniform distribution of vorticity of mixed signs—a distinguishing feature of a fully developed parabolic flow (see Ref. 30).

The coherence exhibited by the jet flow is, in effect, stronger than that existing in a conventional mixing layer because the base flow that carries the vorticity field slows down as r^{-1} from the origin, where $r=|z|$. Our results reveal the existence of a distinct interface between the vortex fluid—the fluid carrying a high concentration of vorticity—and the nonvortex fluid, that is, the one devoid of vorticity. The essential nonstationarity of this interface leads to the well-known phenomenon of intermittency, in which finite turbulent effects manifest themselves at the outer contour of the jet for only a fraction of time. Nonetheless, as a consequence of the far-field effect of vorticity, fluid from surroundings is entrained into the jet core. Thus, whereas fluctuations in the flowfield are affected by diffusion inside the jet within the vortex fluid, they are essentially independent of viscous forces in the nonvortex fluid surrounding the jet.

These effects are also evident in the velocity vector fields displayed in Fig. 5. In particular, the effects of entrainment are displayed in the diagrams at $T=16$ and $T=26$ by the relatively large negative velocities in the far field, pointing toward the jet axis. We should emphasize here that these observations were gathered from a two-dimensional, time-dependent solution. Thus, they resemble the actual turbulent flow only on a qualitative basis and at a stage where three-dimensional phenomena are of negligible influence.

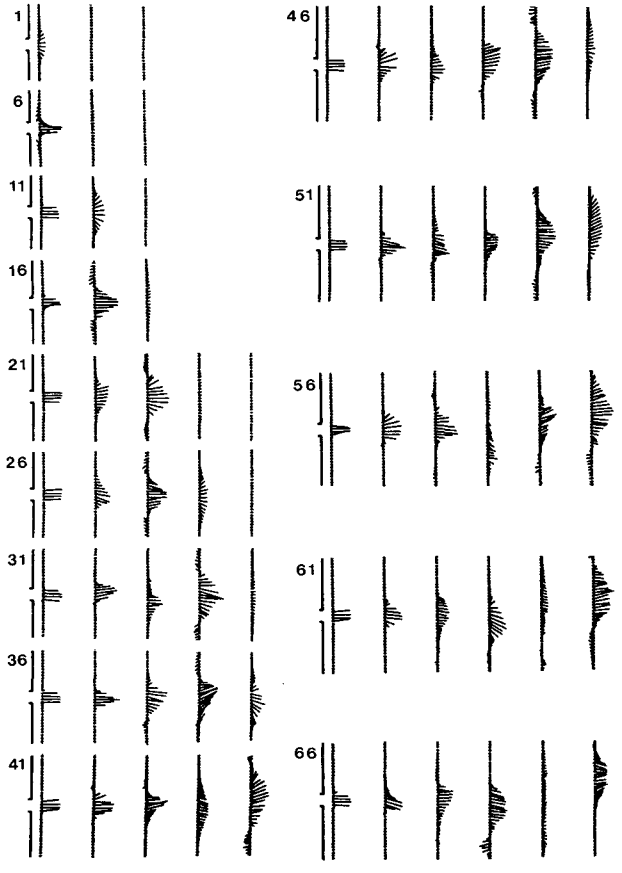

Fig. 5 Velocity profiles corresponding to Fig. 4; numbers as in Fig. 3.

Flame

To study the effect of inflammation, two cases were considered. In the first, the flame was initiated by ignition at the center of the orifice; in the second, combustion was initiated across its full cross section. In both cases, the normal burning speed was taken as $S_u=0.02u_i$, while the volumetric expansion

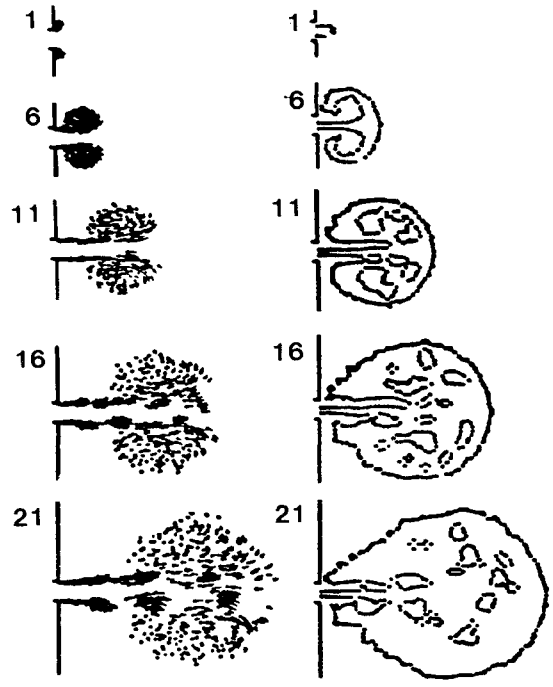

Fig. 6 Development of vorticity field and the corresponding flame fronts associated with the inflammation of a turbulent jet following ignition at the center of the orifice. $Re=10{,}000$; $S_u=0.02u_i$; $\beta=v_b/v_u=4$; numbers as in Fig. 3.

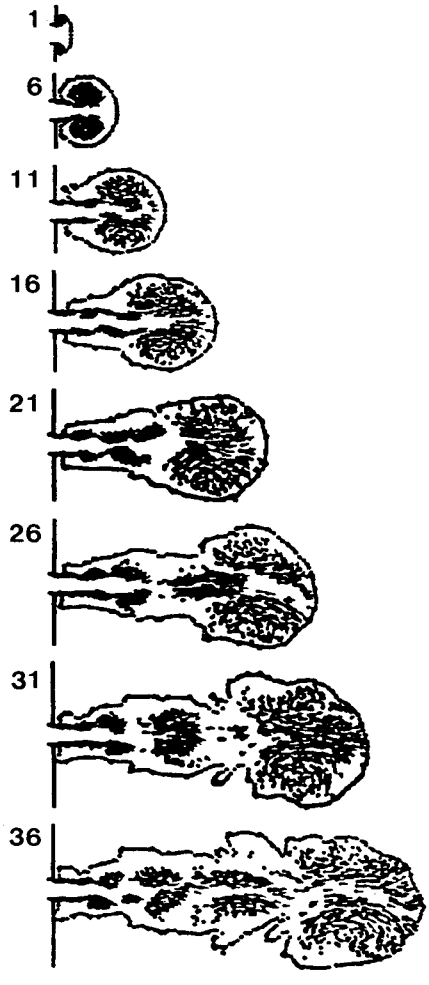

Fig. 7 Development of vorticity field and progress of the flame associated with the formation of a turbulent torch generated by a jet of hot products issuing from an orifice. Parameters same as in Fig. 6; numbers as in Fig. 3.

ratio (in effect, the temperature ratio across the flame front) $\beta = 4$.

The results of the first case are presented in Fig. 6. The first column displays the development of the vorticity field, while the second shows the corresponding progress of flame fronts. As evident here, the rate of recirculation, at $Re = 10{,}000$ for which these results were obtained, is sufficiently high to cause entrainment of reactants into the products at the core of the jet, creating islands of unreacted fluid. The effects of volumetric expansion are manifested by the swelling of the vortex fluid, which can be clearly observed by comparing the vorticity vector fields of Fig. 6 with those of Fig. 4 at corresponding times.

The second case, representing the effects of a turbulent torch igniting a combustible atmosphere, is depicted in Fig. 7. The flame front establishes itself at the outer contour of the vortex fluid whose structure is dominated by large-scale eddies, as in the case of an inert jet. However, the expansion due to the exothermicity of the combustion process causes the vortex blobs to spread apart, thereby reducing the effects of coherence between them. Nonetheless, the recirculation due to these eddies is of major importance in consolidating the field of combustion products, keeping the flame front at the boundary of the vortex structure.

Conclusions

Our studies revealed the following features of jet formation and inflammation:

1) At initial stages, the propagation of a turbulent jet is dominated by the formation of large-scale eddies and the essentially inviscid interaction between them.

2) The spread of the jet is manifested by the growth of its vorticity field—a process due essentially to the effects of diffusion and convection. The dynamic effects of the jet extend into the surroundings, far beyond the boundary of its vorticity field.

3) The flowfield is stratified into a vortex fluid, i.e., the fluid carrying a high concentration of vorticity, and the nonvortex fluid, that is, one devoid of vorticity, associated with a distinct inerface between the two. It is the intrinsic instability of this interface that provides a deterministic explanation for the well-known stochastic phenomenon of intermittency.

4) The engulfment of fluid from the surroundings into the core of the jet is, in essence, an inviscid process induced by the recirculation due to large-scale eddies—the effective components of the jet structure. The entrainment of this fluid within the vortex fluid is, however, a viscous process affected by diffusion.

5) The growth of the turbulent jet structure consists of three stages: formation of eddies, pairing of eddies with the same sign of circulation, and pairing of eddies of opposite signs, the last being associated with fluctuating displacements of the vortex field transversely to the jet axis.

6) The inflammation of a jet and the spreading of the jet flame are also dominated by the action of large-scale eddies, although the coherence between them is impaired as a consequence of the volumetric expansion due to the exothermicity of the combustion process. The recirculation promoted by the eddies furnishes the basic mechanism for the entrainment of reactants from the surroundings and the consolidation of products within the core of the turbulent jet.

Acknowledgments

This work was supported by the Office of Energy Research, Basic Energy Sciences Division of the U.S. Department of Energy under Contract No. W-7405-ENG-48, the National Science Foundation under Grant CPE 81-15163, and the National Aeronautics and Space Administration Lewis Research Center under Grant NAG 3-131.

References

[1]Chen, D. Y., Ghoniem, A. F., and Oppenheim, A. K., "Experimental and Theoretical Study of Combustion Jet Ignition," NASA CR 168139, 1983.

[2]Cetegen, B., Teichman, K., Weinberg, F.J., and Oppenheim, A.K., "Performance of a Plasma Jet Igniter," *SAE 80042*, Warrendale, PA, 1980.

[3]Oppenheim, A. K., Teichman, K., Hom, K., and Stewart, H. E., "Jet Ignition of an Ultra-lean Mixture," *SAE Transactions*, Vol. 87, No. 3, SAE, Warrendale, PA, 1978, pp. 2146-2428.

[4]Oppenheim, A. K. et al., "A Cinematographic Study of Combustion in an Enclosure Fitted with a Reciprocating Piston," in *Stratified Charge Engines, I*, Mechanical Engineering Conference Publications 1976-11, London, Nov. 1976, pp. 127-135.

[5]Chorin, A. J., "Numerical Studies of Slightly Viscous Flow," *Journal of Fluid Mechanics*, Vol. 57, Pt. 4, June 1973, pp. 785-796.

[6]Chorin, A. J., "Vortex Sheet Approximation of Boundary Layers," *Journal of Computational Physics*, Vol. 27, June 1978, pp. 428-442.

[7]Chorin, A. J., "Vortex Models and Boundary Layer Instability," *SIAM Journal of Scientific and Statistical Computing*, Vol. 1, March 1980, pp. 1-24.

[8]Ghoniem, A. F., Chorin, A. J., and Oppenheim, A. K., "Numerical Modeling of Turbulent Combustion in Premixed Gases," *Proceedings of the 18th Symposium (International) on Combustion*, The Combustion Institute, Pittsburgh, PA, 1981, pp. 1375-1383.

[9]Ghoniem, A. F., Chorin, A. J., and Oppenheim, A. K., "Numerical Modeling of Turbulent Flow in a Combustion Tunnel," *Philosophical Transactions of the Royal Society of London*, A304, 1982, pp. 303-325.

[10]Chorin, A. J., "Flame Advection and Propagation Algorithms," *Journal of Computational Physics*, Vol. 35, March 1980, pp. 1-11.

[11]Majda, A., "Equations for Low Mach Number Combustion," Report PAM-112, Center for Pure and Applied Mathematics, Universtiy of California, Berkeley, Nov. 1982.

[12]Brown, G. L. and Roshko, A., "On Density Effects and Large Scale Structure in Turbulent Mixing Layers," *Journal of Fluid Mechanics*, Vol. 64, July 1974, pp. 775-816.

[13]Roshko, A., "Structure of Turbulent Shear Flows: A New Look," *AIAA Journal*, Vol. 14, Oct. 1976, pp. 1349-1357.

[14]Brown, G. L. and Thomas, A. W., "Large Structure in a Turbulent Boundary Layer," *Physics of Fluids,* Vol. 20, No. 10, 1977, pp. S243-S252.

[15]Delcourt, B. A. G. and Brown, G. L., "The Evolution and Emerging Structure of a Vortex Sheet in an Inviscid and Viscous Fluid Modeled by a Point Vortex Method," *Proceedings of the 2nd Symposium on Turbulent Shear Flow*, edited by Bradbury et al., Imperial College, London, 1979.

[16]Papailou, D. D. and Lykoudis, P.S., "Turbulent Vortex Streets and the Entrainment Mechanism of the Turbulent Wake," *Journal of Fluid Mechanics*, Vol. 62, Jan. 1974, pp. 11-31.

[17]Browand, F. K. and Laufer, J., "The Role of Large Scale Structure in the Initial Development of Circular Jets," *Proceedings of the 4th Biennial Symposium on Turbulence in Liquid,* Univ. of Missouri, Rolla, Sept. 22-24, 1975.

[18]Patnaik, P. C., Sherman, F. S., and Corcos, G. M. "Numerical Simulation of Kelvin-Helmholtz Waves of Finite Amplitude," *Journal of Fluid Mechanics,* Vol. 73, Jan. 1976, pp. 215-240.

[19]Corcos, G. M. and Sherman, F. S., "Vorticity Concentration and the Dynamics of Unstable Free Shear Layers," *Journal of Fluid Mechanics,* Vol. 73, Jan. 1976, pp. 241-264.

[20]Ashurst, W. T., "Numerical Simulation of Turbulent Mixing Layers via Vortex Dynamics," *Proceedings of the First Symposium on Turbulent Shear Flows,* edited by F. Durst et al., Springer-Verlag, Berlin, 1979, pp. 402-413.

[21]Hald, O. H. and Del Prete, V. M., "Convergence of Vortex Methods for Euler Equations," *Mathematics of Computation,* Vol. 32, July 1978, pp. 791-809.

[22]Hald, O. H., "Convergence of Vortex Methods for Euler's Equations II," *SIAM Journal of Numerical Analysis,* Vol. 16, Oct.1979, pp. 726-755.

[23]Beale, J. T. and Majda, A., "Vortex Methods, II: Higher Order Accuracy in Two and Three Dimensions," *Mathematics of Computation,* Vol. 39, No. 159, 1982, pp. 28-52.

[24]Beale, J. T. and Majda, A., "Rates of Convergence for Viscous Splitting of the Navier-Stokes Equations," *Mathematics of Computation,* Vol. 37, No. 156, 1982, pp. 243-260.

[25]Ghoniem, A. F., Marek, C. J., and Oppenheim, A. K., "Modeling Interface Motion of Combustion (MIMOC), a Computer Code for Two-Dimensional Unsteady Turbulent Combustion," NASA 2132, 1983.

[26]Noh, W. T. and Woodward, P., "SLIC (Simple Line Interface Calculation)," *Proceedings of the 5th International Conference on Numerical Methods in Fluid Mechanics*, Springer-Verlag, Berlin, 1976, pp. 330-339.

[27]Sethian, J., "An Analysis of Flame Propagation," LBL-14125, 1982, Lawrance Berkeley Laboratory, Berkeley, CA.

[28]Baker, R., "The 'Cloud-in-Cell' Technique Applied to the Roll-Up of Vortex Sheets," *Journal of Computational Physics,* Vol. 31, April 1979, pp. 76-95.

[29]Leonard, A., "Vortex Methods for Flow Simulation," *Journal of Computational Physics*, Vol. 37, 1980, pp. 289-335.

[30]Ghoniem, A. F. and Sherman, F. S., "Grid-Free Simulation of Diffusion Using Random Walk," *Journal of Computational Physics*, 1985 (in press).

AIAA Meetings of Interest to Journal Readers*

Date	Meeting (Issue of *AIAA Bulletin* in which program will appear)	Location	Call for Papers†
1986			
April 29-May 1	**AIAA Annual Meeting** (Feb.)	Hyatt Regency Crystal City Arlington, VA	
May 12-14	**AIAA/ASME 4th Fluid Mechanics, Plasma Dynamics and Lasers Conference** (March)	Colony Square Hotel Atlanta, GA	Aug. 85
May 19-21	**AIAA/ASME/ASCE/AHS 27th Structures, Structural Dynamics and Materials Conference** (March)	Marriott Hotel San Antonio, TX	May 85
June 2-4	**AIAA/ASME 4th Thermophysics and Heat Transfer Conference** (April)	Sheraton-Boston Hotel Boston, MA	Sept. 85
June 9-11	**AIAA 4th Applied Aerodynamics Conference** (April)	Inter-Continental Hotel San Diego, CA	Sept. 85
June 16-20‡	**10th U.S. National Congress on Theoretical and Applied Mechanics**	Austin, TX	
July 9-11	**AIAA 10th Aeroacoustics Conference** (May)	Seattle, WA	Oct. 85

*For a complete listing of AIAA meetings, see the current issue of the *AIAA Bulletin*.
†Issue of *AIAA Bulletin* in which Call for Papers appeared.
‡Co-sponsored by AIAA. For program information, write to: AIAA Meetings Department, 1633 Broadway, New York, NY 10019.